AIAA JOURNAL
Vol. 32, No. 10, October 1994

# Probability Approach for Prediction of Corrosion and Corrosion Fatigue Life

D. Gary Harlow* and Robert P. Wei†
*Lehigh University, Bethlehem, Pennsylvania 18015*

**A probability approach for life prediction is developed and illustrated through a simplified model for the pitting corrosion and corrosion fatigue crack growth in aluminum alloys in aqueous environments. A method for estimation of the cumulative distribution function (CDF) for the lifetime is demonstrated by using an assumed CDF for each key random variable (RV). The basic aim of this approach is to make predictions for the lifetime, reliability, and durability beyond the range of typical data by integrating the CDFs of the individual RVs into a mechanistically based model. The contribution of each key RV is considered, and its significance is assessed. Thus, the usefulness of probability-based modeling is demonstrated. It is noted that physically realistic parameters were assumed for the illustrations. As such, the results from analysis of the model qualitatively agree quite well with experimental observations. However, these results should not be construed to represent behavior in actual systems. Because of these assumptions, confidence levels for the predictions are not addressed.**

## Introduction

PITTING corrosion and corrosion fatigue crack initiation and growth in aluminum alloys are recognized as significant degradation mechanisms that affect the reliability, durability, and integrity of both military and commercial aircraft. A quantitative approach for defining suitable inspection intervals and mandating repairs is needed for an effective management of an aging fleet of aircraft. Also, a comparable methodology is needed for assessing the durability and integrity of new airframe components and structures.

Prediction of reliability or durability requires statistically accurate estimates of material response for loading and environmental conditions typically not included within available experimental observations. The desired estimates often involve extrapolations in time by factors of 10 or more. These can be made only if the fundamental random variables (RVs) that affect the failure processes can be identified and modeled by appropriate failure mechanisms. Thus, a mechanistically based probability model for the lifetime must be developed.

The goal of this effort is to make estimates of the lifetime of an aluminum alloy subjected to a variety of conditions, such as temperature, stress level, and frequency. It is recognized that failure can occur by corrosion per se or by corrosion-assisted fatigue crack nucleation and growth. The model here is focused on pitting and subsequent corrosion fatigue crack nucleation and growth in the alloy in an aqueous environment, for example, condensation in joints. The contribution from each RV to the variability in lifetime is assessed. The main sources of variability addressed in the illustrative model are those from the mechanical and corrosion properties of the alloy and the electrochemical behavior induced by the environment. Furthermore, the role of the major deterministic variables also are considered. These include thermal effects and loading conditions. The significance of the deterministic and random quantities is evaluated by using parameter values and assumed probability distributions that are typical in experimental observations.

## Development of the Model

One of the essential aspects in the development of a mechanistically based probability model is the formulation of the damage process. The model must contain a relatively accurate representation of the damage mechanism as a function of all of the key deterministic and random variables. The damage process to be considered in this effort is pitting corrosion and corrosion fatigue in aluminum alloys. Specifically, the model is motivated by the effect of environment on the surface of a rivet hole in an alloy sheet, which would be bare, that is, no cladding or protective coating. For convenience, the damage is assumed to begin by the formation of a corrosion pit on the rivet hole surface. As pitting corrosion continues to a critical pit size, a corrosion fatigue surface (thumbnail) crack nucleates from it. The surface crack ultimately transitions into a through (or through-thickness) crack that grows until some prescribed inspection or failure criterion is realized. For modeling convenience, the damage process is divided into three regimes, and then the corresponding lifetime $t_f$ can be computed as the sum of $t_{ci}$, the time required for a nucleated pit to grow and for a surface crack to initiate from it, $t_{tc}$, the time required for the surface crack to grow into a through crack, and $t_{cg}$, the time for a through crack to grow to a prescribed critical length, given as part of a failure criterion. Thus, the time-to-failure $t_f$ is given by the following:

$$t_f = t_{ci} + t_{tc} + t_{cg} \tag{1}$$

The assumed model is illustrated schematically in Fig. 1. Randomness associated with material properties and their sensitivity to the environmental and loading conditions are explicitly contained in the model. However, because detailed mechanistic models for pitting corrosion and corrosion fatigue are yet to be developed fully, well-established empirical features are incorporated into the model.

The key RV of interest in probability modeling is the time-to-failure $t_f$. The goal is to find the cumulative distribution function (CDF) for $t_f$. It is the CDF that accounts for scatter in an RV and that allows for identification, estimation, and prediction of reliability. Since $t_f$ is assumed to be the sum given in Eq. (1), the task is to find analytical expressions for $t_{ci}$, $t_{tc}$, and $t_{cg}$ and subsequently to compute the CDF for $t_f$.

### Pitting Corrosion Model

In keeping with Kondo[1] and Kondo and Wei,[2] the following simplified pit growth is assumed in which the pit remains hemispherical in shape and grows at a constant volumetric rate $dV/dt$ given by

$$\frac{dV}{dt} = 2\pi a^2 \frac{da}{dt} = \frac{MI_{P_0}}{nF\rho} \exp\left(-\frac{\Delta H}{RT}\right) \tag{2}$$

Received Oct. 12, 1993; revision received May 2, 1994; accepted for publication May 6, 1994. 

*Professor of Mechanics, Department of Mechanical Engineering and Mechanics, 19 Memorial Drive West.

†Paul B. Reinhold Professor of Mechanics, Department of Mechanical Engineering and Mechanics, 19 Memorial Drive West.

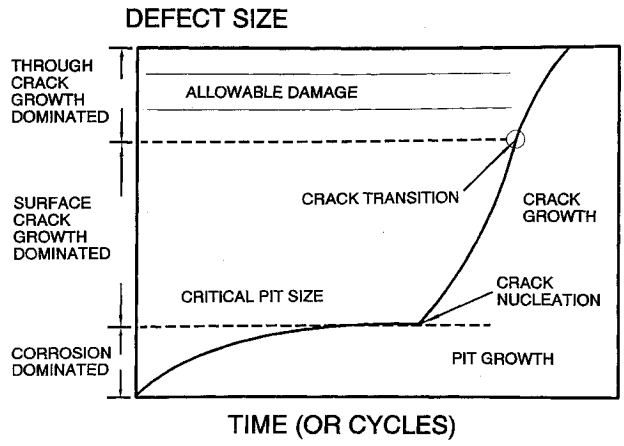


**Fig. 1 Schematic representation of pitting corrosion and corrosion fatigue.**

where $a$ is the pit radius, $M$ is the molecular weight of the material, $n$ is the valence, $F = 96{,}514$ C/mole is Faraday's constant, $\rho$ is density, $\Delta H$ is the activation energy, $R = 8.314$ J/mole-K is the universal gas constant, $T$ is the absolute temperature, and $I_{P_0}$ is the pitting current coefficient. It is manifest that $t_{ci}$ can be found by simple integration of the right-hand side in Eq. (2) to be given by

$$t_{ci} = \frac{2\pi nF\rho}{3MI_{P_0}}(a_{ci}^3 - a_0^3)\exp\left(\frac{\Delta H}{RT}\right) \tag{3}$$

where $a_{ci}$ is the pit radius at which a crack is initiated, and $a_0$ is the initial pit radius.

The pit radius at which a crack is initiated $a_{ci}$ can be expressed in terms of the threshold driving force $\Delta K_{\text{th}}$ via the crack growth mechanism.[1,2] For the sake of simplicity and computational expediency, the surface crack remains semicircular in shape, and the stress intensity factor range is given by

$$\Delta K_s = \frac{2.2}{\pi}K_t\Delta\sigma\sqrt{\pi a} \tag{4}$$

where $\Delta\sigma$ is the far-field stress range, $K_t$ is the stress concentration factor resulting from the circular rivet hole, and the factor of $2.2/\pi$ is for a semicircular flaw in an infinite plate. Again following Kondo,[1] the surface crack is assumed to nucleate from a hemispherical corrosion pit when $\Delta K_s$ increases to $\Delta K_{\text{th}}$. The corresponding crack length that satisfies this condition is easily found to be

$$a_{ci} = \pi\left(\frac{\Delta K_{\text{th}}}{2.2K_t\Delta\sigma}\right)^2 \tag{5}$$

Consequently, the expression for $t_{ci}$ is found by substituting Eq. (5) into Eq. (3).

### Corrosion Fatigue Model

Since the environmental effect on aluminum alloys is expected to be at its maximum in typical aircraft applications, the standard power law form for the corrosion fatigue growth rate $(da/dN)_c$ is assumed to be the mechanistically based model. Thus,

$$\left(\frac{da}{dN}\right)_c = C_c(\Delta K)^{n_c} \tag{6}$$

where $n_c$ represents the mechanistic dependence, specifically the functional dependence, of the crack growth rate on the driving force $\Delta K$, and it is taken to be deterministic. The coefficient $C_c$ is assumed to be an RV that reflects the variability in material properties and the contributions of microstructural and environmental parameters to that variability.

The driving force $\Delta K$ is considered to be of two different forms according to whether the crack is a surface crack or a through crack. For a surface crack, $\Delta K$ equals $\Delta K_s$ given in Eq. (4), and it remains so until the crack can be modeled as a through crack. When the crack becomes a through crack, $\Delta K$ is assumed to be equal to $\Delta K_{tc}$, which has the following form:

$$\Delta K_{tc} = F_{tc}\left(\frac{a}{r_0}\right)\Delta\sigma\sqrt{\pi a} \tag{7}$$

where $r_0$ is the radius of the rivet hole. Bowie[3] numerically evaluated $F_{tc}(a/r_0)$ for ratios of $a/r_0$ in the interval [0, 10] for an infinite plate under uniaxial tension containing a circular hole with a single through crack emanating from the hole perpendicular to the loading axis. The numerical values can be fit empirically, to within graphical resolution, by the function given by

$$F_{tc}\left(\frac{a}{r_0}\right) = \frac{0.865}{(a/r_0)+0.324} + 0.681 \tag{8}$$

which is suitable for analytical computations. The remaining question concerning the driving force $\Delta K$ is that of the transition from a surface crack to a through crack. It is assumed that the transition occurs at the crack length $a_{tc}$, which is defined by equating the geometry-dependent functions from Eqs. (4) and (7). Thus, the transition crack length $a_{tc}$ is the solution of

$$F_{tc}\left(\frac{a_{tc}}{r_0}\right) = \frac{2.2}{\pi}K_t \tag{9}$$

which is easily found to be

$$a_{tc} = r_0\left[\frac{0.865}{(2.2/\pi)K_t - 0.681} - 0.324\right] \tag{10}$$

The final computation to be completed is for $t_{tc}$ and $t_{cg}$ using Eq. (6).

First consider the computation for the time between crack initiation and transition to a through crack $t_{tc}$. Substituting Eq. (4) into Eq. (6) yields a simple differential equation in that the variables $a$ and $N$ can be separated, and an explicit solution can be found. Assuming that $N = \nu t$, then,

$$t_{tc} = \frac{2(\sqrt{\pi})^{n_c}\left[(\sqrt{a_{ci}})^{2-n_c} - (\sqrt{a_{tc}})^{2-n_c}\right]}{\nu(n_c-2)C_c(2.2K_t\Delta\sigma)^{n_c}} \tag{11}$$

if $n_c \neq 2$. For aluminum alloys, typically $n_c \neq 2$, and consequently it is sufficient to only consider this case. Now consider the computation for the time between the transition to a through crack and the final crack size. Combining Eq. (7) and (8) and substituting them into Eq. (6) yields

$$t_{cg} = \int_{a_{tc}}^{a_f} \frac{1}{\nu C_c(\Delta\sigma\sqrt{\pi})^{n_c}}\left(\frac{0.324r_0 + a}{1.086r_0\sqrt{a} + 0.681(\sqrt{a})^3}\right)^{n_c} da \tag{12}$$

where $a_f$ is the final crack size. The integral in Eq. (12) can be evaluated explicitly only when $n_c$ is an integer. This assumption will be used for the ensuing computations. Thus, all of the random times that comprise $t_f$ in Eq. (1) have been described, and the CDF for $t_f$ can be computed given explicit values for the deterministic parameters and RVs. This model was used to demonstrate several important modeling concepts; however, the results are based on assumed

parameters and should not be construed as indicators of the response in real airframe structures.

## Selection of Deterministic and Random Variables

### Deterministic Variables

The motivating problem for this example is the fuselage pressurization-depressurization cycling of an aircraft. The detailed problem of interest is the behavior of an aluminum alloy, used for the fuselage, near a typical rivet hole that is in an aqueous environment. Table 1 contains the list of the deterministic variables and their values that are used in the numerical computations. Although some of these could be considered as RVs, they are assumed to be deterministic for this effort. Most of the values in the table are self-explanatory; however, a few comments are in order. The values for the frequency $\nu$ are selected to represent long haul ($\nu$ = 2 cycles/day) and short haul ($\nu$ = 10 cycles/day) flights. The temperature values are selected to cover a reasonable range of operating temperatures, and $\Delta H$ of 50 kJ/mole is a typical value for aluminum alloys.[4] The applied stresses $\Delta\sigma$ are typical of the design stress range for many of the aluminum alloys used in fuselages. Finally, the value of 2.6 was selected for the stress concentration factor $K_t$ to reflect an experimental condition in which a specimen approximately 40 mm in width containing a circular hole of radius 3 mm in the center undergoes uniaxial tension.

The characterization of the final crack length $a_f$ is more difficult because it is associated with the failure condition, the experimental termination criterion, or the replacement or repair condition of a component. Certainly, there are ways in which to define $a_f$ so that it is not deterministic, and indeed, these may be more suited to reality. However, herein $a_f$ is assumed to be deterministic. Such an assumption corresponds to specifying an inspection limit for $a_f$.

### Random Variables

For this model, the randomness is attributed to the following four variables: the pitting current coefficient $I_{P_0}$, the initial pit size $a_0$, the corrosion fatigue crack growth coefficient $C_c$, and the fatigue crack growth threshold $\Delta K_{th}$. None of these RVs are stochastic processes, i.e., the RVs are chosen to be mechanistically and statistically independent of time. The parameter $C_c$ reflects variability in material properties, more specifically its resistance to fatigue crack growth and environmental sensitivity. The initial pit size $a_0$ represents material and manufacturing quality. The fatigue threshold $\Delta K_{th}$ is also a function of the material quality. The final RV $I_{P_0}$ reflects the scatter associated with the electrochemical reaction for pit growth.

To select an appropriate CDF for each of these RVs, extensive experimental and statistical testing is needed. Because the CDFs are not known, the Weibull CDF is assumed, for simplicity, for all of the RVs. The Weibull CDF is chosen because it is sufficiently robust to provide an adequate estimate for the statistical character of the RVs; see Barlow and Proschan,[5] for example. The three-parameter Weibull CDF is chosen and is given by

$$F(x) = 1 - \exp\left\{-\left[\frac{x-\gamma}{\beta}\right]^{\alpha}\right\}, \qquad x \geq \gamma \tag{13}$$

where $\alpha$ is the shape parameter, $\gamma$ is the location parameter or minimum value, and $\beta$ is the scale parameter. The parameters in the Weibull CDF are related to physical quantities in the following way: $\alpha$ is characteristic of the variability in the RV; $[\gamma + \beta\Gamma(1 + 1/\alpha)]$ is the mean value $\mu$ of the RV, where $\Gamma(x)$ is the incomplete gamma function; and $\gamma$ is the minimum value of the RV. It should be noted, however, that the choice of the Weibull CDF is not an essential feature of the model development, and in fact, any CDF could be used.

Table 2 contains the assumed values for the parameters in each Weibull CDF. For actual components or systems, more realistic CDFs and parameter estimates must be obtained through accurate experimental and statistical modeling.

**Table 1 Deterministic parameters used in the model for an aluminum alloy**

| Parameter | Aluminum |
|---|---|
| Density $\rho$, gm/m$^3$ | $2.7 \times 10^6$ |
| Molecular weight $M$ | 27 |
| Valence $n$ | 3 |
| Activation energy $\Delta H$, kJ/mole | 50 |
| Temperature $T$, K | 273, 293, 313 |
| Applied stress $\Delta\sigma$, MPa | 80, 90, 100 |
| Stress concentration factor $K_t$ | 2.6 |
| Frequency $\nu$, cycles/day | 2, 10 |
| Crack growth exponent $n_c$ | 3 |
| Radius of rivet hole $r_0$, mm | 3 |
| Final crack size $a_f$, mm | 3 |

**Table 2 Weibull parameters used in the model for an aluminum alloy**

| Random variable | $\alpha$ | $\beta$ | $\gamma$ | $\mu$ |
|---|---|---|---|---|
| Initial pit radius $a_0$, m | 12 | $5.0 \times 10^{-7}$ | $1.5 \times 10^{-6}$ | $1.98 \times 10^{-6}$ |
| Fatigue coefficient $C_c$, m/cycle, (MPa$\sqrt{\text{m}}$)$^{-3}$ | 8 | $3.5 \times 10^{-10}$ | 0 | $3.30 \times 10^{-10}$ |
| Pitting current constant $I_{P_0}$, C/s | 1 | 0.25 | 0.25 | 0.5 |
| Threshold driving force $\Delta K_{th}$, MPa$\sqrt{\text{m}}$ | 10 | 2.365 | 0.25 | 2.5 |
| | 10 | 2.891 | 0.25 | 3.0 |
| | 10 | 3.416 | 0.25 | 3.5 |

## Computation of the CDF for the Time to Failure

The computation of the CDF $F(t)$ for $t_f$ is, in principle, straightforward since the time-to-failure is a sum of three RVs, as given in Eq. (1). However, $t_{ci}$, $t_{tc}$, and $t_{cg}$ are functions of the underlying RVs. The CDF for $t_f$ is found, therefore, by an application of the standard change-of-variables theorem for multidimensional RVs. The simplest form of the result can be found in most standard probability texts; for example, Blake.[6] A more advanced treatment containing engineering applications is given in Harlow and Delph.[7] For completeness, the technique for computing $F(t)$ is outlined next.

Recall the pertinent geometrical values in Table 1. Then from Eq. (10), $a_{tc}$ is found to be 1.3 mm. This value for $a_{tc}$ is in the range of thicknesses of aluminum alloy sheets used in typical aircraft fuselages, that is, between 1 and 2 mm. The slight difference from the actual sheet thickness is due to the simplistic assumption given in Eq. (9) in which the geometrical factors in the different forms of the driving force are equated. Some of the difference may be accounted for in the selection of the value for $K_t$. For example, a decrease of only 10% in the value of $K_t$ results in an increase of over 30% in $a_{tc}$. The preceding value for $a_{tc}$ is deemed to be accurate for the following computations. Given the numerical value for $a_{tc}$ and a value of 3 for $n_c$, then $t_{cg}$, from Eq. (12), explicitly is

$$t_{cg} = \frac{1}{\nu C_c (\Delta\sigma\sqrt{\pi})^3}\left\{-4.353 - \frac{0.0532}{\sqrt{a_f}} + \frac{0.00383\sqrt{a_f}}{(0.00478 + a_f)^2} - \frac{3.228\sqrt{a_f}}{(0.00478 + a_f)} + 44.132 \arctan(14.46\sqrt{a_f})\right\} \tag{14}$$

If the assumed value of 3 mm is inserted for $a_f$, then $t_{cg}$ is further simplified to

$$t_{cg} = \frac{4.987}{\nu C_c (\Delta\sigma\sqrt{\pi})^3} \tag{15}$$

Substituting Eqs. (3), (5), (12), and (16) into Eq. (1) and inserting the numerical values for the fixed deterministic parameters yields an expression for $t_f$:

$$t_f = \frac{6.064 \times 10^{10} \exp(\Delta H/RT)}{I_{P_0}} \left\{ 8.853 \times 10^{-4} \left( \frac{\Delta K_{th}}{\Delta\sigma} \right)^6 - a_0^3 \right\} + \frac{[0.192\Delta\sigma/\Delta K_{th} - 0.751]}{\nu C_c (\Delta\sigma)^3} \tag{16}$$

In (16), notice the explicit occurrence of the four RVs and the deterministic parameters which assume a range of values. To simplify the notation, let $B_1 = C_c$, $B_2 = I_{P_0}$, $B_3 = \Delta K_{th}$, and $B_4 = a_0$. Then Eq. (16) becomes

$$t_f = \frac{6.064 \times 10^{10} \exp(\Delta H/RT)}{B_2} \left\{ 8.853 \times 10^{-4} \left( \frac{B_3}{\Delta\sigma} \right)^6 - B_4^3 \right\} + \frac{[0.192\Delta\sigma/B_3 - 0.751]}{\nu B_1 (\Delta\sigma)^3} \tag{17}$$

so that $t_f$ is a mapping from $\boldsymbol{R}^4$ into $\boldsymbol{R}^1$, where $\boldsymbol{R}^D$ represents a $D$-dimensional real space. The computation of the probability density function (PDF) for $t_f$ is, again, a straightforward application of the change-of-variables theorem for multiple integrals in which an augmentation is needed. The augmentation is necessary because a change of variables requires a mapping from one $D$-dimensional space into another. Let the augmented variables be defined by $N_1 = t_f$, $N_2 = B_2$, $N_3 = B_3$, and $N_4 = B_4$; thus, $\boldsymbol{H}$: $(B_1, B_2, B_3, B_4) \rightarrow (N_1, N_2, N_3, N_4)$ satisfies the conditions of the change-of-variables theorem. Since the last three components of the mapping are trivial, the inverse of $\boldsymbol{H}$ is rather easy to compute, and $B_1$ can be found explicitly to be as follows:

$$B_1 = \frac{[0.192\Delta\sigma/N_3 - 0.751]}{\nu(\Delta\sigma)^3 \left\{ N_1 - \frac{6.064 \times 10^{10} \exp(\Delta H/RT)}{N_2} \left[ 8.853 \times 10^{-4} (N_3/\Delta\sigma)^6 - N_4^3 \right] \right\}} \tag{18}$$

Likewise the Jacobian of the inverse is given by

$$J = \left| \frac{\partial B_1}{\partial N_1} \right| = \frac{[0.192\Delta\sigma/N_3 - 0.751]}{\nu(\Delta\sigma)^3 \left\{ N_1 - \frac{6.064 \times 10^{10} \exp(\Delta H/RT)}{N_2} \left[ 8.853 \times 10^{-4} (N_3/\Delta\sigma)^6 - N_4^3 \right] \right\}^2} \tag{19}$$

Finally, the CDF for $t_f$ can be expressed as a fourfold integral.

$$F(t) = \int_0^t \int_0^\infty \int_0^\infty \int_0^\infty |J| f_{B_1, B_2, B_3, B_4} [B_1(n_1, n_2, n_3, n_4), n_2, n_3, n_4] \, dn_1 \, dn_2 \, dn_3 \, dn_4 \tag{20}$$

where $f_{B_1, B_2, B_3, B_4}$ is the joint PDF for $B_1$, $B_2$, $B_3$, and $B_4$. The only possible solution is numerical, and numerical solutions of multidimensional integrals are nontrivial. Nevertheless, Eq. (20) is sufficiently well behaved that standard procedures are applicable, and the numerical accuracy is well within the model precision. For another engineering application of this type of probability analysis, see Harlow and Wei.[8]

## Results and Discussion

The deterministic parameters such as frequency $\nu$, far-field stress range $\Delta\sigma$, or temperature $T$ are often used to accelerate the failure process to decrease the time required for testing. These are, therefore, the key external variables for time extrapolation. The influence of each of these variables now can be considered collectively or in turn. Similarly, the contribution of each of RV to the variability and the overall lifetime can be assessed. Analytical sensitivity studies are very useful in constructing an experimental design for an experimental test plan and in refining the assumed mechanistic model for the failure process.

The influence of the applied stress range $\Delta\sigma$ on the predicted distribution $F(t)$ for the time-to-failure $t_f$ is shown in Fig. 2, for a frequency of 10 cycles/day. The CDF is spread over a broader range as $\Delta\sigma$ decreases, which indicates that the variability is increasing. The variability shown in this figure is a reflection of the scatter associated with all of the RVs. Another observation, which is consonant with experimental results, is that $F(t)$ is stochastically ordered in that, for fixed $t$, $F(t)$ strictly decreases as $\Delta\sigma$ decreases. In other words, for a fixed value of $F(t)$, the random life $t_f$ decreases as the applied stress range increases. The median life, which is estimated from the 50 percentile of $F(t)$, from smaller to larger values, differs by a factor of about 2.5 for the given range of applied stresses. The reason for the rather abrupt and almost vertical lower tail for $F(t)$ is that there is a minimum life associated with the assumed model. In other words, there is some amount of time that will transpire before failure is statistically possible. Obviously, the minimum life is a function of the applied stress. The behavior of $F(t)$ when $\nu$ is lowered to 2 cycles/day is very similar to that shown in Fig. 2. One difference is that the range of the median failure times is more narrow, differing by only a factor of about 2. The only substantial difference is that the median times to failure are now larger by a factor of about 3.

Along with the CDF for $t_f$, Fig. 3 shows the CDF for the time-to-initiation $t_{ci}$, i.e., the time of the failure process spent in pitting corrosion up to crack initiation; see Eq. (3). This figure graphically displays the contribution of the two major types of damage accumulation, namely, pitting corrosion and corrosion fatigue. Notice that the amount of scatter is roughly the same order of magnitude for the two CDFs for $t_f$ but that it is quite large for the CDF for $t_{ci}$.

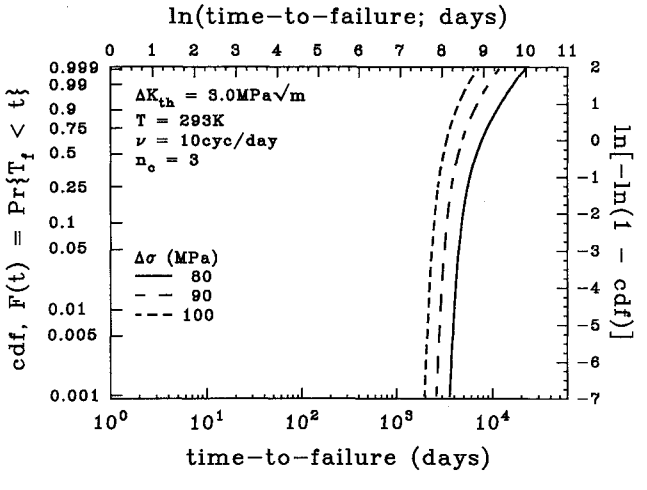


**Fig. 2 Influence of applied stress on the CDF for the time to failure at 293 K and 10 cycles/day.**

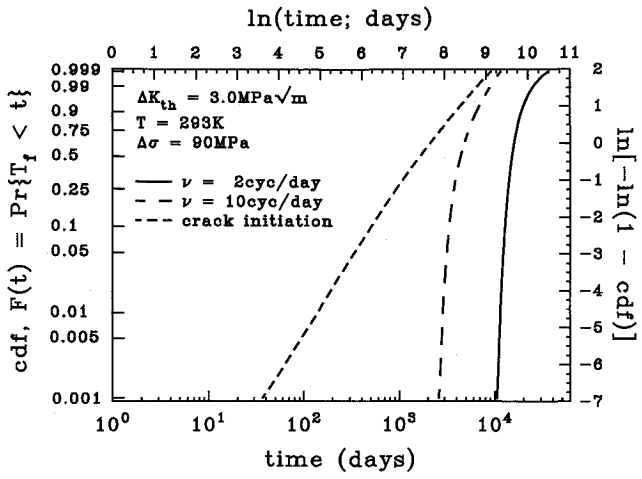


Fig. 3 Relative contribution of the time to initiation and the time of crack growth on the CDF for the time to failure at 293 K and 90 MPa.

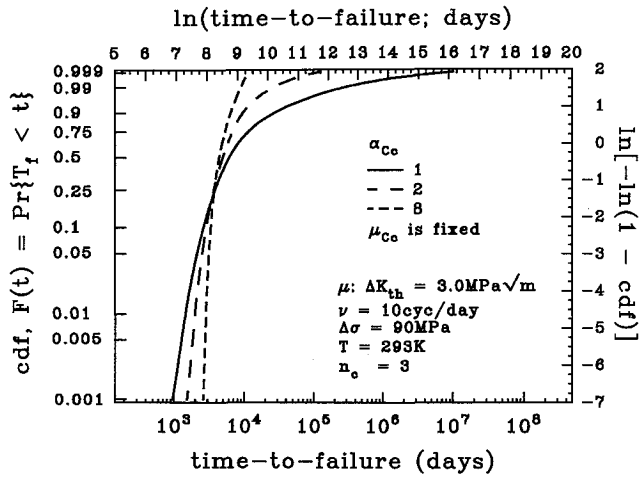


Fig. 6 Influence of the variability in the corrosion fatigue crack growth coefficient on the CDF for the time to transition at 293 K and 90 MPa.

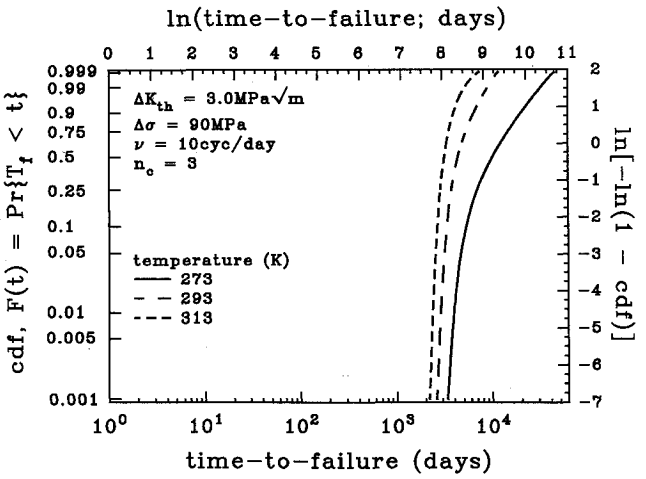


Fig. 4 Influence of temperature on the CDF for the time to failure at 10 cycles/day and 90 MPa.

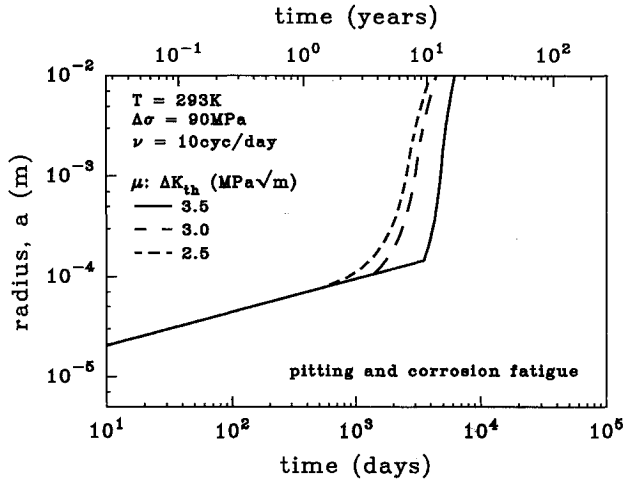


Fig. 7 Influence of the mean threshold driving force on the flaw growth during pitting corrosion and corrosion fatigue at 10 cycles/day, 293 K, and 90 MPa.

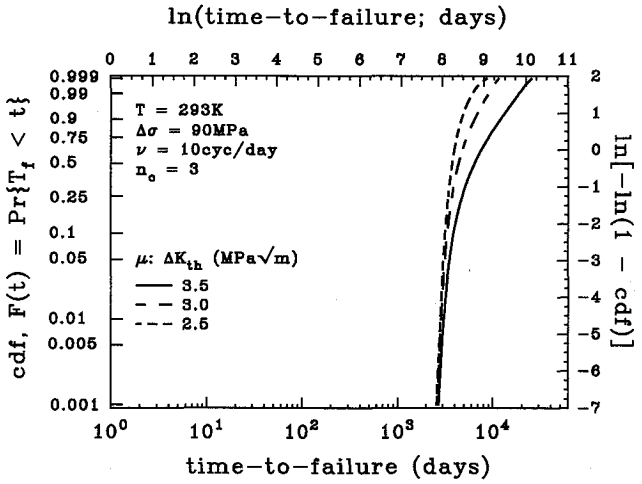


Fig. 5 Influence of the mean threshold driving force on the CDF for the time to failure at 10 cycles/day, 293 K, and 90 MPa.

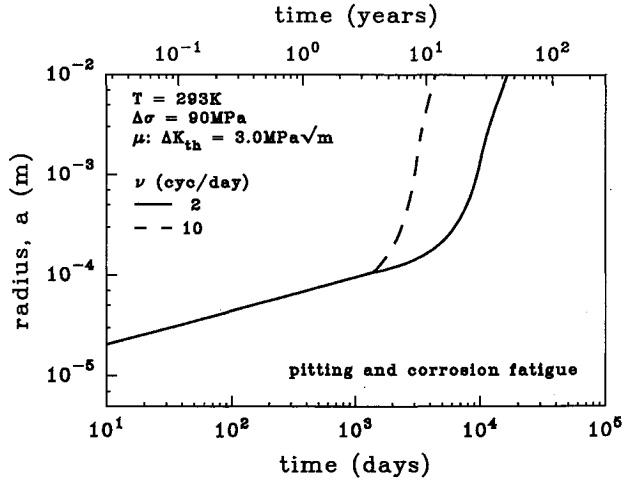


Fig. 8 Influence of frequency on the flaw growth during pitting corrosion and corrosion fatigue at 293 K and 90 MPa.

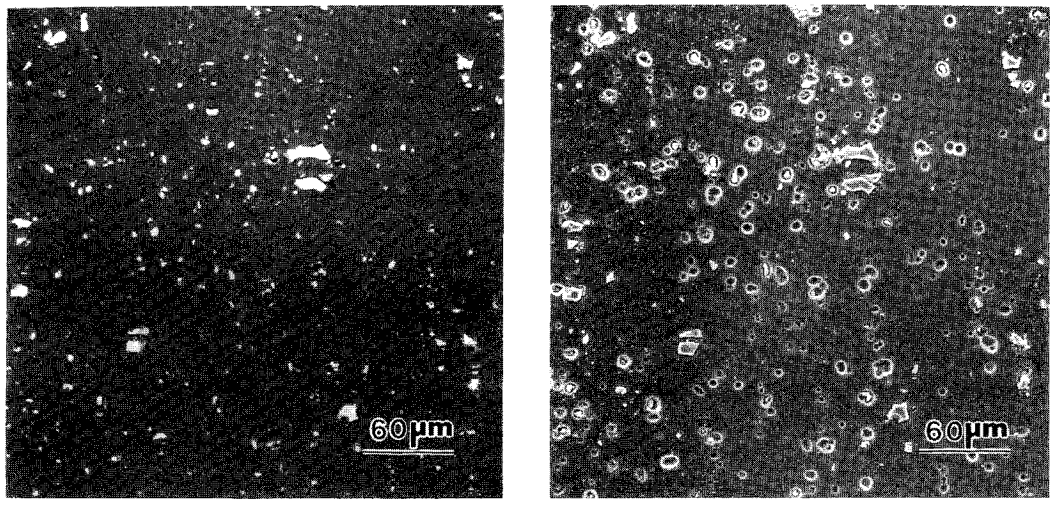


**Fig. 9 Typical scanning electron micrographs of 2024-T3 aluminum alloy before and after three-day exposure to 0.5 molar NaCl (aerated) at room temperature.**

The large variability in $t_{ci}$ is directly attributable to the large scatter assumed for the pitting current coefficient $I_{P_0}$. When $\nu = 10$ cycles/day, a large fraction, about 40%, of the median life is expended in pit growth. When $\nu = 2$ cycles/day, this fraction drops to about 10%. Also, notice that the upper tail of the CDF for $t_f$ when $\nu = 10$ cycles/day is highly dominated by pitting corrosion. The same observation holds, but to a much lesser extent, when $\nu = 2$ cycles/day. On the other hand, the lower tail behavior is clearly dominated by corrosion fatigue.

Figure 4 is an example of the influence of the temperature $T$, where $T$ varies from 273 to 313 K for $\nu = 10$ cycles/day. For the assumed model, the only place in which $T$ plays a role is in pitting corrosion; see Eq. (3). Thus, as $T$ varies, $F(t)$ is affected in the upper tail portion. This behavior is vividly reflected by the CDF for $T = 273$ K whose upper tail is nearly identical to the corresponding CDF for $t_{ci}$ for probabilities above 0.75. However, the difference between the median live of $t_{ci}$ and $t_f$ increases as $T$ increases. As in Fig. 3, the corrosion fatigue dominated lower tail portion of the CDFs are virtually identical in shape, and the relatively small difference in translation is due to the difference in the temperature-dependent median values.

Since $\Delta K_{\text{th}}$ is such a critical RV for $t_f$, through its influence on both $t_{ci}$ and $t_{tc}$, its effect is displayed in Fig. 5. The mean for $\Delta K_{\text{th}}$ varies from 2.5 to 3.5 MPa$\sqrt{\text{m}}$. As the mean increases, the scatter increases. Again, as in Fig. 3, the upper tail behavior of $F(t)$ approaches the upper tail of the CDF for $t_{ci}$. The other striking feature is that all of the CDFs have a nominally identical minimum life. Even difference in the medians varies only by about a factor of 1.7. Thus, for the given range of values for the mean of $\Delta K_{\text{th}}$, there is not an overly abundant effect on the CDF for $t_f$.

Another very important RV is $C_c$, which is directly associated with the quality of the alloy. The role of $C_c$ on $t_f$ is shown in Eq. (17); however, its contribution to the overall variability in $t_f$ is displayed in Fig. 6. The mean of $C_c$ is fixed for all of the cases considered, but the variability in $C_c$ is changed. The coefficient of variation for $C_c$ ranges from 15 to 100%. It is manifest that as the scatter increases for $C_c$, the scatter also increases dramatically for $t_f$. Furthermore, the increase in scatter in $C_c$ has an adverse effect on the high-reliability region of the CDF for $t_f$. That is, as the scatter in $C_c$ increases, the estimated lifetime at a given level of high reliability, i.e., the lower tail of the CDF, decreases. Thus, the quality of the alloy as reflected in $C_c$ is crucial to high-reliability applications.

## Observations

To assure that this single flaw model is physically consistent, the rate of flaw growth for the pitting corrosion must be considerably less than the rate of corrosion fatigue growth for times beyond the time to initiation. Figures 7 and 8 show the mean flaw radius vs time for the different mechanisms of growth. The linear portion of the curve is precisely characteristic of the flaw growth via pitting corrosion. The distinct transition results from the condition assumed in Eq. (4), which is tantamount to assuming that the rate of crack growth is greater than the rate of pit growth at crack initiation. This restriction implicitly assumes that the pit must be sufficiently large that crack growth is essentially instantaneous and dominant at initiation. It should be noted, however, that this assumption is valid only for certain conditions. For instance, at high frequencies cracks may initiate from pits very early in the life, but the rate of pitting corrosion growth may be greater than the ensuing rate of growth for small cracks. For the example herein, the assumption should be valid. Nevertheless, note that for $\nu = 2$ cycles/day on Fig. 8 the transition is not that distinct, which implies that the extremes for the validity of the model are being reached. The other inflection point in the graph represents the transition from a small crack to a through crack. When the through crack growth begins, $\Delta K_{tc}$ is slightly less than $\Delta K_s$, and consequently the flaw growth rate is reduced a small amount. The times-to-initiation and the times-to-failure generated by this model are at least reasonable approximations.

Even so, the single flaw model for aluminum alloys may not be as accurate as desired. It has been observed by Chen et al.[9] that in an aluminum alloy there is substantial interaction between corrosion pits during nucleation and growth; see Fig. 9. Therefore, the proper model for pitting corrosion and crack growth must include a nearest neighbor interaction and effect. This will be the thrust of a future effort.

One of the most critical aspects of the mechanistically based probability modeling is the identification of all of the variables, deterministic and random. Certainly, this includes an extensive design and execution of experiments to develop mechanistic models for damage accumulation in terms of these variables and quantification of their CDFs. Greater accuracy in modeling directly results in greater accuracy in reliability estimations.

## Summary

A probability model has been developed for pitting corrosion and corrosion fatigue crack growth for aluminum alloys in aqueous environments. This type of model is required for making accurate estimates or predictions of the service life at times or loading conditions that are well beyond the range that contains typical supporting data. This model is based on the growth of a single dominant flaw from a pit to a small surface crack and then into a through

crack. The flaw growth is governed by a model for electrochemical reaction controlled pit growth in conjunction with a power law (Paris-Erdogan) relationship for corrosion fatigue crack growth.

The probabilistic contributions from the material properties on the times to failure were assessed as functions of applied stress, loading frequency, and temperature. The results are qualitatively consistent with typical observations. This effort illustrates that probabilistic modeling is well suited for making long-term reliability predictions. Also, it facilitates parametric analyses that are not possible with many statistical approaches. It is apparent that the mechanistic understanding of corrosion fatigue crack growth is still incomplete and that the CDFs for the key RVs have not been characterized adequately. Nevertheless, it has been shown that the probability aspects must be integrated throughout the modeling process. They cannot be added ex post facto to a mechanistic study or an experimental effort. Additional research is needed to further develop the necessary information and understanding.

## Acknowledgments

This research was supported in part by the Federal Aviation Administration under Grant 92-G-006 and the Air Force Office of Scientific Research under Grant F49620-93-1-0426.

## References

[1]Kondo, Y., "Prediction of Fatigue Crack Initiation Life Based on Pit Growth," *Corrosion*, Vol. 45, No. 1, 1989, pp. 7–11.

[2]Kondo, Y., and Wei, R. P., "Approach on Quantitative Evaluation of Corrosion Fatigue Crack Initiation Condition," *International Conference on Evaluation of Materials Performance in Severe Environments*, EVAL-MAT 89, Vol. 1, Iron and Steel Institute of Japan, 1989, pp. 135–142.

[3]Bowie, O. L., "Analysis of an Infinite Plate Containing Radial Cracks Originating at the Boundary of an Internal Circular Hole," *Journal of Mathematics and Physics*, Vol. 35, No. 1, 1956, pp. 60–71.

[4]Foley, R. T., "Localized Corrosion of Aluminum Alloys—A Review," *Corrosion*, Vol. 42, No. 5, 1986, pp. 277–288.

[5]Barlow, R. E., and Proschan, F., *Statistical Theory of Reliability and Life Testing*, 2nd ed., To Begin With, Silver Spring, MD, 1981, pp. 226–253.

[6]Blake, I. F., *An Introduction to Applied Probability*, Wiley, New York, 1979, pp. 206–219.

[7]Harlow, D. G., and Delph, T. J., "The Numerical Solution of Random Initial-Value Problems," *Mathematics and Computers in Simulation*, Vol. 33, No. 3, 1991, pp. 243–258.

[8]Harlow, D. G., and Wei, R. P., "A Mechanistically Based Approach to Probability Modeling for Corrosion Fatigue Crack Growth," *Engineering Fracture Mechanics*, Vol. 45, No. 1, 1993, pp. 79–88.

[9]Chen, G., Gao, M., and Wei, R. P., "Constituent Induced Pitting Corrosion for a 2024-T3 Aluminum Alloy," *Corrosion* (submitted for publication).